Articles

Dimeric Rhodium μ-Silylene and μ-η^2-Silyl Complexes: Catalytic Silicon−Silicon Bond Formation and X-ray Structures of $[\{Pr^i_2PCH_2CH_2PPr^i_2\}Rh]_2(\mu\text{-}SiRR')_2$ (R = R′ = Ph and R = Me, R′ = Ph) and $[\{Pr^i_2PCH_2CH_2PPr^i_2\}Rh(H)]_2(\mu\text{-}\eta^2\text{-}H{-}SiMe_2)_2$†

Lisa Rosenberg,*,‡ Michael D. Fryzuk, and Steven J. Rettig§

Department of Chemistry, University of British Columbia, 2036 Main Mall, Vancouver, British Columbia, Canada V6T 1Y6

Received July 29, 1998

The stoichiometric and catalytic reactions of secondary silanes with the rhodium hydride bridged dimer $[(dippe)Rh]_2(\mu\text{-}H)_2$ (**1**; dippe = 1,2-bis(diisopropylphosphino)ethane) are described. The reaction of **1** with Ph_2SiH_2 results in the formation of the bis(μ-silylene) complex $[(dippe)Rh]_2(\mu\text{-}SiPh_2)_2$ (**2a**); a similar reaction ensues upon addition of $MePhSiH_2$ or $Me^pTolSiH_2$ (^{p}Tol = *p*-tolyl) to **1** except that the bis(silylene) complexes exist as a mixture of *cis* and *trans* stereoisomers. Dimethylsilane reacts with **1** to generate the dinuclear complex $[(dippe)Rh(H)]_2(\mu\text{-}\eta^2\text{-}H{-}SiMe_2)_2$ (**4d**). The hydride dimer acts as a catalyst precursor for the dimerization of excess Ph_2SiH_2 to tetraphenyldisilane ($Ph_2SiHSiHPh_2$). A catalytic cycle is proposed that consists of dinuclear intermediates.

Introduction

The activation of Si−H bonds by transition-metal complexes, originally the focus of research into homogeneously catalyzed hydrosilation,[1−3] has come under renewed scrutiny to determine its role in dehydrogenative silicon coupling reactions.[4−6] Silicon−silicon bond formation catalyzed by d^0 metallocene catalysts is now known to occur via σ-bond metathesis reactions at mononuclear centers,[7] but despite long-standing precedence for the activity of late-transition-metal catalysts toward this reaction,[8−10] no mechanism of dehydrogenative silicon−silicon coupling as catalyzed by the late transition metals has been conclusively established. A catalytic cycle based on oxidative-addition and reductive-elimination steps at a metal hydride center has become generally accepted (Scheme 1),[11,12] but while individual steps in this cycle have been observed in stoichiometric reactions of various mononuclear, late transition-metal systems,[4] for no one system have all the steps been observed to occur stoichiometrically. Studies of silane dehydropolymerization using late-metal catalysts have not ruled out the possibility of dinuclear intermediates.

We report here the catalytic activity of the dinuclear rhodium hydride complex $[(dippe)Rh]_2(\mu\text{-}H)_2$ (**1**; dippe = 1,2-bis(diisopropylphosphino)ethane) toward the dehydrogenative dimerization of diphenylsilane.[13,14] A series of dinuclear rhodium μ-silylene and μ-η^2-silyl complexes, whose synthesis and characterization are described, are implicated as intermediates in this process: their reactivity provides evidence for all steps of a catalytic cycle responsible for silicon−silicon coupling, occurring at a dinuclear center.

Results and Discussion

Synthesis, Characterization and Reactivity of Dimeric, μ-Silylene Complexes. Addition of 2 equiv

† This article is dedicated to the memory of Steven J. Rettig.

‡ Present address: Department of Chemistry, University of Manitoba, Winnipeg, Manitoba, Canada R3T 2N2.

§ Professional Officer: UBC X-ray Crystal Structural Laboratory. Deceased October 27, 1998.

(1) Chalk, A. J.; Harrod, J. F. *J. Am. Chem. Soc.* **1965**, *87*, 16.
(2) Harrod, J. F.; Chalk, A. J. In *Organic Syntheses Via Metal Carbonyls*; Wender, I., Pino, P., Eds.; Wiley: New York, 1977; p 690.
(3) Ojima, I. In *The Chemistry of Organic Silicon Compounds*; Patai, S., Rappoport, Z., Eds.; Wiley: New York, 1989; p 1479.
(4) Tilley, T. D. *Comments Inorg. Chem.* **1990**, *10*, 37.
(5) Yamashita, H.; Tanaka, M. *Bull. Chem. Soc. Jpn.* **1995**, *68*, 403.
(6) Sharma, H. K.; Pannell, K. H. *Chem. Rev.* **1995**, *95*, 1351.
(7) Woo, H.; Walzer, J. F.; Tilley, T. D. *J. Am. Chem. Soc.* **1992**, *114*, 7047.
(8) Brown-Wensley, K. A. *Organometallics* **1987**, *6*, 1590.
(9) Lappert, M. F.; Maskell, R. K. *J. Organomet. Chem.* **1984**, *264*, 217.
(10) Ojima, I.; Inaba, S.; Kogure, T. *J. Organomet. Chem.* **1973**, *55*, C7.
(11) Curtis, M. D.; Epstein, P. S. *Adv. Organomet. Chem.* **1981**, *19*, 213.
(12) Other mechanisms for this reaction have been advanced that are based on the insertion of terminal silylene ligands into M−Si bonds: Corey, J. Y. In *Advances in Silicon Chemistry*; Larson, G. L., Ed.; JAI Press: Greenwich, CT, 1991; Vol. 1, p 327. Hengge, E.; Weinberger, M. *J. Organomet. Chem.* **1993,** *443*, 167.
(13) The activity of **1** for this catalytic dimerization was reported previously in a communication; mechanistic details were unavailable at that time.[14]
(14) Fryzuk, M. D.; Rosenberg, L.; Rettig, S. J. *Organometallics* **1991**, *10*, 2537.

10.1021/om980651s CCC: $18.00
Publication on Web 02/13/1999

Scheme 1

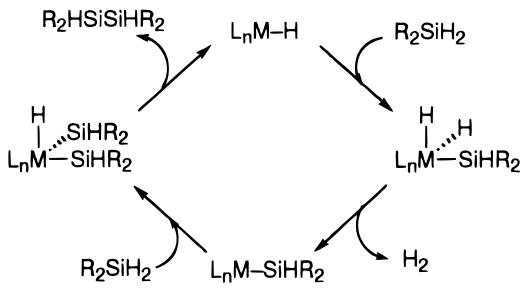

of diphenylsilane to [(dippe)Rh]$_2$(μ-H)$_2$ (**1**) results in the formation of the bis(μ-silylene) complex [(dippe)Rh]$_2$(μ-SiPh$_2$)$_2$ (**2a**) with simultaneous loss of 3 equiv of hydrogen (eq 1).[15,16] This complex, soluble in aromatic

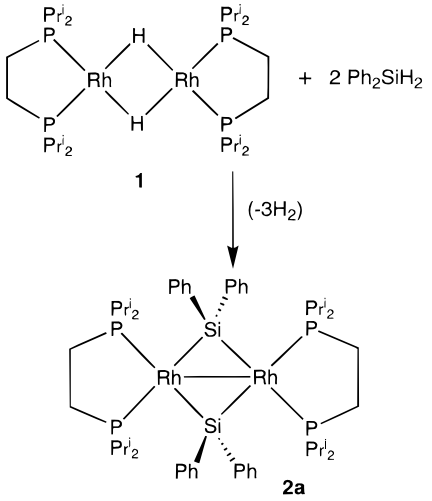

(1)

solvents and sparingly soluble in aliphatic hydrocarbon and halogenated solvents, is air- and moisture-sensitive in solution but is air-stable in the solid state for short periods of time (hours). The ^{31}P{^{1}H} NMR spectrum of **2a** shows a center-symmetric doublet of multiplets typical of an AA′A″A‴XX′ system; the pattern is similar to those observed for other dinuclear rhodium complexes in this system, including that of **1**.[17,18] The ^{1}H NMR spectrum of **2a** is consistent with a solution structure in which the rhodium atoms have a square-planar arrangement of ligands, with substituents on the tetrahedral silicons projecting into and out of the plane.

X-ray diffraction analysis of a single crystal of **2a** confirmed the dimeric structure of this molecule with bridging silylene groups. Two views of the molecular structure of **2a** are shown in Figure 1, crystallographic data are given in Table 1, and pertinent bond distances and angles are shown in Table 2 . Each rhodium center in the dimer has a distorted-square-planar geometry (if one ignores the Rh—Rh bond); when the dimer is viewed down the Rh—Rh axis, the two square planes are skewed relative to each other, with an angle between the two mean square planes of 46.95°. Loss of planarity due to puckering of the two five-membered Rh(dippe) chelate rings does not affect the C_2 axis running through both Si atoms. The observed diamagnetism of **2a** requires a formal single bond between the two rhodium atoms, and this is borne out by the Rh—Rh separation of 2.921(2) Å and the acute silylene bridge angles of 77.25(8) and 76.57(7)°. The Si—Si distance across the dinuclear rhodium center is approximately 3.71 Å,[19] which precludes any interaction between the two silicons. The dimensions of this structure are consistent with those generally observed for dimeric M_2Si_2 complexes.[20]

Complex **2a** is relatively inert, being unreactive toward CO and C_2H_4, but it does react with hydrogen. Solutions of **2a** in hexanes or toluene placed under an atmosphere of hydrogen react to give [(dippe)Rh]$_2$(μ-H)(μ-η^2-H—SiPh$_2$) (**3a**) plus diphenylsilane, as determined by ^{1}H and ^{31}P{^{1}H} NMR spectroscopy. The dihydride dimer **1** is not observed in these reactions; this is in keeping with the observation that addition of hydrogen to **3a** does not cause the elimination of diphenylsilane.[21] Thus, the addition of 1 equiv of diphenylsilane to **1** is an irreversible reaction. The reaction of complex **2a** with excess diphenylsilane will be discussed in the section describing catalytic results.

The methylphenylsilylene analogue of **2a**, [(dippe)Rh]$_2$(μ-SiMePh)$_2$ (**2b**), was isolated as an orange powder. The ^{31}P{^{1}H} spectrum of **2b** indicates the formation of two products in this reaction; these are geometric isomers arising from the potentially *cis* or *trans* disposition of the Si—Me (or Si—Ph) groups across the Rh_2Si_2 plane (eq 2).

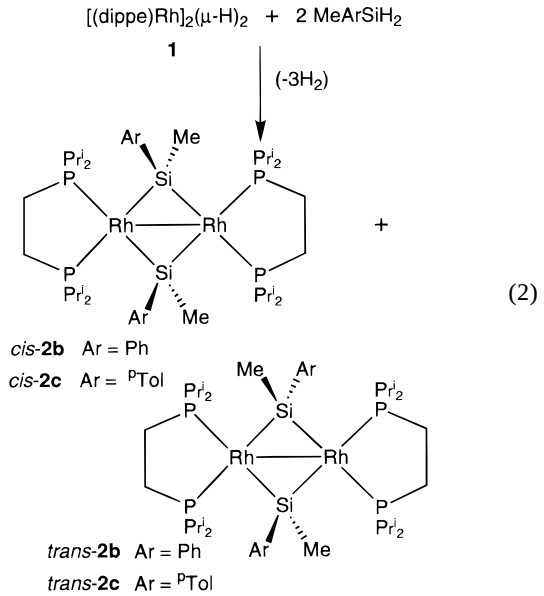

(2)

The ^{1}H and ^{31}P{^{1}H} NMR spectra of **2b** did not allow peak assignments for the *cis* and *trans* isomers, and the two could not be separated by fractional crystallization. The extremely low solubility of these compounds has hampered study of this isomerism, preventing determi-

(15) **2a** can also be prepared by addition of 1 equiv of diphenylsilane to [(dippe)Rh]$_2$(μ-H)(μ-η^2-H-SiPh$_2$) (**3a**).[16]

(16) Fryzuk, M. D.; Rosenberg, L.; Rettig, S. J. *Organometallics* **1996**, *15*, 2871.
(17) Fryzuk, M. D.; Jones, T.; Einstein, F. W. B. *Organometallics* **1984**, *3*, 185.
(18) Piers, W. E. Thesis, University of British Columbia, 1988.
(19) The coordinates for the molecular structure of **3a** were entered into the Chem 3D Plus program through a Molecule Editor using the Cache system by Techtronix, and the Si—Si distance was calculated using the Molecule Editor.
(20) Anderson, A. B.; Shiller, P.; Zarate, E. A.; Tessier-Youngs, C. A.; Youngs, W. J. *Organometallics* **1989**, *8*, 2320.
(21) Rosenberg, L. Ph.D. Thesis, University of British Columbia, 1993.

Table 1. Crystallographic Data[a]

	2a	*trans*-**2b**	**4d**
formula	$C_{52}H_{84}P_4Rh_2Si_2$	$C_{42}H_{80}P_4Rh_2Si_2$	$C_{32}H_{80}P_4Rh_2Si_2$
fw	1095.11	970.97	850.86
color, habit	brown, prism	yellow-orange, prism	yellow, prism
cryst syst	monoclinic	triclinic	orthorhombic
space group	*C*2/*c* (No. 15)	$P\bar{1}$ (No. 2)	$P2_12_12_1$ (No. 19)
a, Å	12.933(6)	11.307(3)	16.869(2)
b, Å	22.538(6)	12.036(3)	19.741(3)
c, Å	18.875(8)	10.798(2)	12.862(2)
α, deg	90	104.26(2)	90
β, deg	99.99(4)	117.38(2)	90
γ, deg	90	67.77(2)	90
V, Å^3	5418(4)	1203.2(5)	4283(2)
Z	4	1	4
ρ_{calcd}, g cm^{-3}	1.342	1.340	1.319
F(000)	2296	510	1800
μ(Mo *K*α), cm^{-1}	7.91	8.81	9.80
cryst size, mm	0.05 × 0.15 × 0.30	0.10 × 0.15 × 0.40	0.20 × 0.25 × 0.45
transmissn factors	0.63−1.00	0.90−1.00	0.93−1.00
scan type	$\omega-2\theta$	$\omega-2\theta$	$\omega-2\theta$
scan range, *ω*, deg	1.21 + 0.35 tan θ	1.00 + 0.35 tan θ	1.31 + 0.35 tan θ
scan speed, deg min^{-1}	16 (up to 9 scans)	16 (up to 9 scans)	32 (up to 9 scans)
data collected	$+h, +k, \pm l$	$+h, \pm k, \pm l$	$+h, +k, +l$
$2\theta_{max}$, deg	55	65	60
cryst decay, %	6.4	negligible	negligible
total no. of rflns	6675	9114	6883
no. of unique rflns	6392	8726	6883
R_{merge}	0.048	0.028	
no. of rflns with $I \geq 3\sigma(I)$	2756	6177	4936
no. of variables	272	227	388
R	0.036	0.030	0.025
R_w	0.028	0.029	0.026
GOF	1.45	1.68	1.18
max Δ/σ (final cycle)	0.16	0.08	0.04
residual density, e Å^{-3}	−0.41 to +0.39	−0.35 to +0.51	−0.34 to +0.28

[a] Conditions and definitions: temperature, 294 K; Rigaku AFC6S diffractometer; Mo Kα (λ = 0.710 69 Å) radiation; graphite monochromator; takeoff angle 6.0°, aperture 6.0 × 6.0 mm at a distance of 285 mm from the crystal; stationary background counts at each end of the scan (scan/background time ratio 2:1); $\sigma^2(F^2) = [S^2(C + 4B)]/Lp^2$ (S = scan rate, C = scan count, B = normalized background count), function minimized $\sum w(|F_o| - |F_c|)^2$, where $w = 4F_o^2/\sigma^2(F_o^2)$; $R = \sum||F_o| - |F_c||/\sum|F_o|$; $R_w = (\sum w(|F_o| - |F_c|)^2/\sum w|F_o|^2)^{1/2}$; GOF = $[\sum w(|F_o| - |F_c|)^2/(m - n)]^{1/2}$ (where m = number of observations, n = number of variables). Values given for R, R_w, and GOF are based on those reflections with $I \geq 3\sigma(I)$.

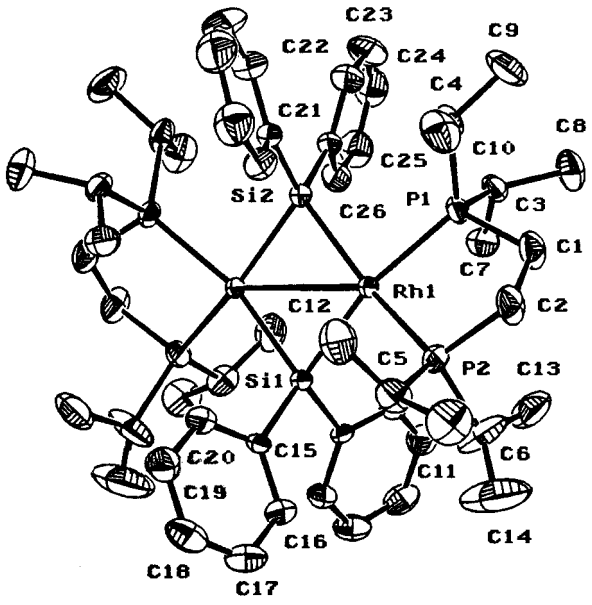

Figure 1. ORTEP view of **2a** (33% probability thermal ellipsoids are shown for the non-hydrogen atoms).

nation of the ratio of isomers formed. However, crystals of the complex suitable for an X-ray diffraction study were obtained by slow evaporation of solvent from a very dilute solution of **2b** in hexanes. The structure obtained was of the *trans* isomer. (See Figure 2 for an ORTEP diagram of *trans*-**2b** and Table 3 for relevant bond distances and bond angles.) The dimensions of the molecular structure of *trans*-**2b** are analogous to those observed for **2a**, except that far less twisting of the two chelate rings relative to each other renders the geometries at rhodium closer to square planar (if one ignores

Table 2. Selected Bond Lengths (Å) and Angles (deg) for 2a[a]

Rh(1)−Rh(1)*	2.921(2)	Rh(1)−P(1)	2.295(2)
Rh(1)−P(2)	2.288(2)	Rh(1)−Si(1)	2.357(2)
Rh(1)−Si(2)	2.054(5)	P(1)−C(1)	1.831(6)
P(1)−C(3)	1.852(6)	P(1)−C(4)	1.886(6)
P(2)−C(2)	1.860(6)	P(2)−C(5)	1.848(6)
P(2)−C(6)	1.864(7)	Si(1)−C(15)	1.911(5)
Si(2)−C(21)	1.898(6)		
Rh(1)*−Rh(1)−P(1)	135.34(4)	Rh(1)*−Rh(1)−P(2)	138.26(5)
Rh(1)*−Rh(1)−Si(1)	51.71(4)	Rh(1)*−Rh(1)−Si(2)	51.37(4)
P(1)−Rh(1)−P(2)	86.34(6)	P(1)−Rh(1)−Si(1)	162.41(5)
P(1)−Rh(1)−Si(2)	86.21(6)	P(2)−Rh(1)−Si(1)	89.45(6)
P(2)−Rh(1)−Si(2)	159.30(5)	Si(1)−Rh(1)−Si(2)	103.09(5)
Rh(1)−P(1)−C(1)	108.3(2)	Rh(1)−P(1)−C(3)	116.0(2)
Rh(1)−P(1)−C(4)	122.2(2)	C(1)−P(1)−C(3)	101.9(3)
C(1)−P(1)−C(4)	102.9(3)	C(3)−P(1)−C(4)	103.0(3)
Rh(1)−P(2)−C(2)	107.7(2)	Rh(1)−P(2)−C(5)	116.4(2)
Rh(1)−P(2)−C(6)	123.1(3)	C(2)−P(2)−C(5)	100.2(3)
C(2)−P(2)−C(6)	102.8(4)	C(5)−P(2)−C(6)	103.5(3)
Rh(1)−Si(1)−Rh(1)*	76.57(7)	Rh(1)−Si(1)−C(15)	121.7(2)
Rh(1)−Si(1)−C(15)*	115.5(2)	C(15)−Si(1)−C(15)*	105.0(4)
Rh(1)−Si(2)−Rh(1)*	77.25(8)	Rh(1)−Si(2)−C(21)	119.8(2)
Rh(1)−Si(2)−C(21)*	114.4(2)	C(21)−Si(2)−C(21)*	108.7(4)

[a] Asterisks denote the symmetry operation $1 - x, y, {}^1/_2 - z$.

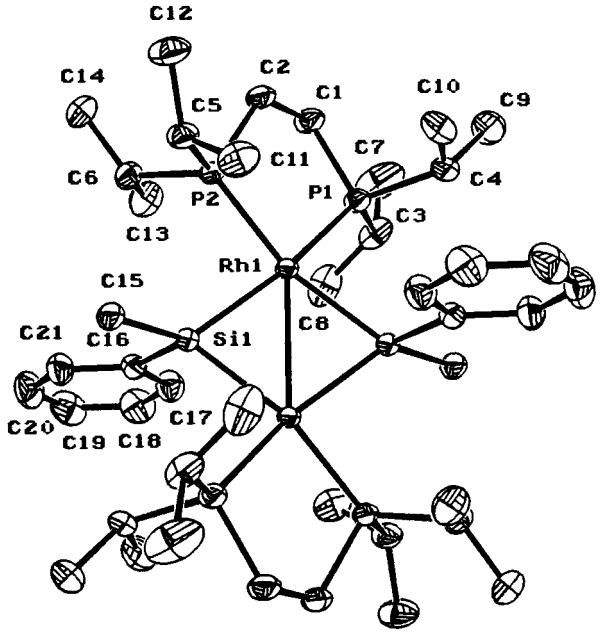

Figure 2. ORTEP view of *trans*-**2b** (33% probability thermal ellipsoids are shown for the non-hydrogen atoms).

Table 3. Selected Bond Lengths (Å) and Angles (deg) for *trans*-2b[a]

Rh(1)−Rh(1)*	2.8925(9)	Rh(1)−P(1)	2.273(1)
Rh(1)−P(2)	2.2760(8)	Rh(1)−Si(1)	2.345(1)
Rh(1)−Si(1)*	2.3531(8)	P(1)−C(1)	1.856(3)
P(1)−C(3)	1.866(3)	P(1)−C(4)	1.856(3)
P(2)−C(2)	1.848(3)	P(2)−C(5)	1.868(3)
P(2)−C(6)	1.865(3)	Si(1)−C(15)	1.908(2)
Si(1)−C(16)	1.902(2)		
Rh(1)*−Rh(1)−P(1)	136.27(2)	Rh(1)*−Rh(1)−P(2)	136.89(2)
Rh(1)*−Rh(1)−Si(1)	52.12(2)	Rh(1)*−Rh(1)−Si(1)*	51.88(2)
P(1)−Rh(1)−P(2)	86.83(3)	P(1)−Rh(1)−Si(1)	160.92(3)
P(1)−Rh(1)−Si(1)*	86.93(3)	P(2)−Rh(1)−Si(1)	87.07(3)
P(2)−Rh(1)−Si(1)*	161.52(2)	Si(1)−Rh(1)−Si(1)*	104.00(3)
Rh(1)−P(1)−C(1)	107.93(8)	Rh(1)−P(1)−C(3)	117.3(1)
Rh(1)−P(1)−C(4)	119.8(1)	C(1)−P(1)−C(3)	101.9(1)
C(1)−P(1)−C(4)	103.9(1)	C(3)−P(1)−C(4)	103.8(1)
Rh(1)−P(2)−C(2)	107.85(8)	Rh(1)−P(2)−C(5)	117.98(9)
Rh(1)−P(2)−C(6)	119.07(9)	C(2)−P(2)−C(5)	101.7(1)
C(2)−P(2)−C(6)	103.9(1)	C(5)−P(2)−C(6)	104.1(1)
Rh(1)−Si(1)−Rh(1)*	76.00(3)	Rh(1)−Si(1)−C(15)	126.37(8)
Rh(1)−Si(1)−C(16)	112.81(8)	Rh(1)*−Si(1)−C(15)	127.01(8)
Rh(1)*−Si(1)−C(16)	111.02(8)	C(15)−Si(1)−C(16)	102.4(1)

[a] Asterisks denote the symmetry operation $1 - x$, $1 - y$, $1 - z$.

the Rh−Rh bond). The single crystal used for the diffraction experiment was dissolved in d_8-toluene and its ^{1}H NMR spectrum recorded, allowing assignment of the peaks due to the *trans* isomer in spectra of mixtures of the two isomers. The other peaks were assigned to the *cis* isomer.

A more soluble *cis*/*trans* isomer pair of the bis(μ-silylene) complex **2** is isolated from the reaction of **1** with 2 equiv of methyl-*p*-tolylsilane (eq 2). Alternatively, the intermediate complex [(dippe)Rh]$_2$(μ-H)(μ-η^2-H−SiMeTol^p) (**3c**), which results from the addition of 1 equiv of methyl-*p*-tolylsilane to **1** and shows details in its ^{1}H and ^{31}P{^{1}H} NMR spectra similar to those seen for [(dippe)Rh]$_2$(μ-H)(μ-η^2-H−SiMePh) (**3b**),[16] reacts with another 1 equiv of methyl-*p*-tolylsilane to produce a mixture of *cis*- and *trans*-**2c**. These isomers are initially formed in a *trans*/*cis* ratio of roughly 2:1. The *trans* isomer (designated *trans* on the basis of comparison

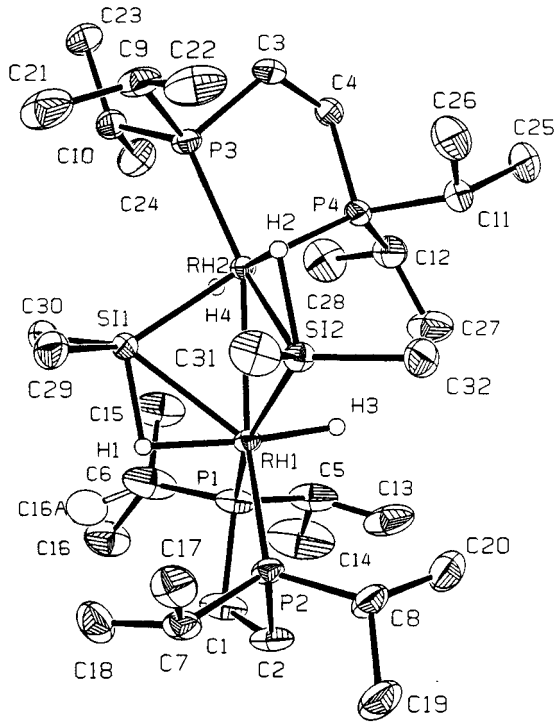

Figure 3. ORTEP view of **4d** (33% probability thermal ellipsoids are shown for the non-hydrogen atoms).

with NMR spectra for *trans*-**2b**) is less soluble than the *cis* isomer and has been isolated pure by fractional crystallization. This isomer is stable in solution at room temperature but when heated to 70 °C or higher begins to convert to the *cis* isomer. At these high temperatures an equilibrium between the isomers is established, with 64% *trans* to 36% *cis* being the highest conversion observed. The approach to a *cis*/*trans* equilibrium from pure *trans*-**2c** at various temperatures was monitored by ^{1}H NMR spectroscopy. However, kinetic analysis of the resulting reaction profiles was prevented by poor reproducibility of the results at specific temperatures and by inconsistent temperature dependence overall.

Synthesis, Characterization and Reactivity of a Dimeric, μ-η²-Silyl Complex. Addition of 2 equiv of dimethylsilane to **1** (or addition of 1 equiv of dimethylsilane to [(dippe)Rh]$_2$(μ-H)(μ-η^2-H−SiMe$_2$) (**3d**)[16]) in hexanes gives a pale, golden yellow solution from which yellow crystals of the formula [(dippe)Rh]$_2$(Me$_2$SiH$_2$)$_2$ (**4d**) can be obtained (eq 3).

$$\underset{\mathbf{1}}{[(\text{dippe})\text{Rh}]_2(\mu\text{-H})_2} + 2\,\text{Me}_2\text{SiH}_2 \xrightarrow{(-\,\text{H}_2)} \underset{\mathbf{4d}}{[(\text{dippe})\text{Rh}]_2(\text{Me}_2\text{SiH}_2)_2} \qquad (3)$$

An X-ray crystallographic study carried out on a single crystal of **4d** confirms the dinuclear structure of this complex. (See Figure 3 for an ORTEP diagram and Table 4 for pertinent bond lengths and bond angles.) The structural relationships between phosphine, silyl, and hydride ligands are more clearly presented in the side and end views of **4d** shown in Figure 4. The

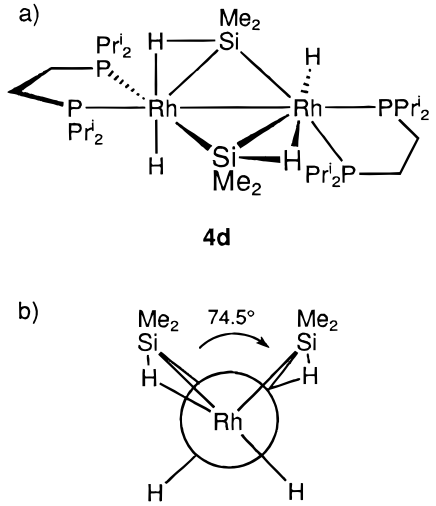

Figure 4. (a) Side and (b) end schematic views of the solid-state structure of **4d**. In the end view, the phosphine ligands have been omitted for clarity.

Table 4. Selected Bond Lengths (Å) and Angles (deg) for 4d

Rh(1)−Rh(2)	2.8575(5)	Rh(1)−P(1)	2.391(1)
Rh(1)−P(2)	2.269(1)	Rh(1)−Si(1)	2.526(1)
Rh(1)−Si(2)	2.337(1)	Rh(1)−H(1)	1.69(4)
Rh(1)−H(3)	1.52(5)	Rh(2)−P(3)	2.279(1)
Rh(2)−P(4)	2.364(1)	Rh(2)−Si(1)	2.324(1)
Rh(2)−Si(2)	2.474(1)	Rh(2)−H(2)	1.70(4)
Rh(2)−H(4)	1.52(4)	Si(1)−C(29)	1.910(5)
Si(1)−C(30)	1.889(5)	Si(1)−H(1)	1.67(5)
Si(2)−C(31)	1.896(5)	Si(2)−C(32)	1.892(5)
Si(2)−H(2)	1.72(4)		
Rh(2)−Rh(1)−P(1)	116.71(3)	Rh(2)−Rh(1)−P(2)	156.18(3)
Rh(2)−Rh(1)−Si(1)	50.69(3)	Rh(2)−Rh(1)−Si(2)	55.81(3)
Rh(2)−Rh(1)−H(1)	92(2)	Rh(2)−Rh(1)−H(2)	83(2)
P(1)−Rh(1)−P(2)	86.72(4)	P(1)−Rh(1)−Si(1)	108.10(4)
P(1)−Rh(1)−Si(2)	162.05(4)	P(1)−Rh(1)−H(1)	89(2)
P(1)−Rh(1)−H(3)	87(2)	P(2)−Rh(1)−Si(1)	128.92(4)
P(2)−Rh(1)−Si(2)	100.56(4)	P(2)−Rh(1)−H(1)	93(1)
P(2)−Rh(1)−H(3)	95(2)	Si(1)−Rh(1)−Si(2)	80.17(4)
Si(1)−Rh(1)−H(1)	41(2)	Si(1)−Rh(1)−H(3)	133(2)
Si(2)−Rh(1)−H(1)	107(2)	Si(2)−Rh(1)−H(3)	76(2)
H(1)−Rh(1)−H(3)	170(2)	Rh(1)−Rh(2)−P(3)	157.52(3)
Rh(1)−Rh(2)−P(4)	113.99(3)	Rh(1)−Rh(2)−H(2)	95(1)
Rh(1)−Rh(2)−H(4)	82(2)	P(3)−Rh(2)−P(4)	86.88(4)
P(3)−Rh(2)−Si(1)	100.37(4)	P(3)−Rh(2)−Si(2)	133.73(4)
P(3)−Rh(2)−H(2)	92(1)	P(3)−Rh(2)−H(4)	91(2)
P(4)−Rh(2)−Si(1)	162.41(4)	P(4)−Rh(2)−Si(2)	105.12(4)
P(4)−Rh(2)−H(2)	94(1)	P(4)−Rh(2)−H(4)	86(2)
Si(1)−Rh(2)−Si(2)	81.52(4)	Si(1)−Rh(2)−H(2)	101(1)
Si(1)−Rh(2)−H(4)	78(2)	Si(2)−Rh(2)−H(2)	44(1)
Si(2)−Rh(2)−H(4)	133(2)	H(2)−Rh(2)−H(4)	177(2)
Rh(1)−Si(1)−Rh(2)	72.06(3)	Rh(1)−Si(1)−C(29)	118.5(2)
Rh(1)−Si(1)−C(30)	125.5(2)	Rh(1)−Si(1)−H(1)	42(2)
Rh(2)−Si(1)−C(29)	125.5(2)	Rh(2)−Si(1)−C(30)	118.6(2)
Rh(2)−Si(1)−H(1)	114(2)	C(29)−Si(1)−C(30)	98.2(2)
C(29)−Si(1)−H(1)	95(2)	C(30)−Si(1)−H(1)	101(2)
Rh(1)−Si(2)−Rh(2)	72.82(3)	Rh(1)−Si(2)−C(31)	125.1(2)
Rh(1)−Si(2)−C(32)	119.6(2)	Rh(1)−Si(2)−H(2)	116(1)
Rh(2)−Si(2)−C(31)	122.3(2)	Rh(2)−Si(2)−C(32)	120.8(2)
Rh(2)−Si(2)−H(2)	43(1)	C(31)−Si(2)−C(32)	97.7(3)
C(31)−Si(2)−H(2)	91(1)	C(32)−Si(2)−H(2)	102(1)
Rh(1)−H(1)−Si(1)	97(2)	Rh(2)−H(2)−Si(2)	93(2)

hydrides attached to rhodium and silicon were located and refined isotropically.

Complex **4d** contains two unsymmetrically bridging silyl groups, each bound to one rhodium center through a covalent Si−Rh bond and to the other rhodium center through a Rh−H−Si three-center, two-electron bond. Each rhodium atom is also bound to one terminal hydride. The geometry around the rhodium centers is roughly octahedral. Two edge-sharing planes, each of which contains the two rhodium atoms, a silicon atom, and the "agostic" hydride associated with that silicon, are almost orthogonal to each other. A dihedral angle of 74.5° gives the dinuclear core a "butterfly" structure (Figure 4).

The observed diamagnetism of $[(dippe)Rh(H)]_2(\mu\text{-}\eta^2\text{-}H{-}SiMe_2)_2$ (**4d**) indicates the presence of a formal, single Rh−Rh bond, consistent with a Rh−Rh separation of 2.8575(5) Å. While the Si−Si separation in **4d** of 3.135 Å[22] is sufficiently long to preclude any bonding interaction (the normal range for a Si−Si single bond is 2.33−2.70 Å[23]), this distance is much shorter than those normally observed for dimeric complexes containing bridging silylene ligands (3.852−4.225 Å[24]). Obviously the shorter distance is due largely to steric considerations in the butterfly-shaped structure, but it does give rise to the possibility of elimination of a silicon−silicon-bonded entity from the dinuclear center. The relevance of this structure to dehydrogenative coupling of silanes catalyzed by **1** is discussed further in the section concerned with the catalytic dimerization of diphenylsilane (*vide infra*).

Features related to the two agostic Si−H bonds in the structure of **4d** are very similar to those observed for the silyl hydride complexes **3a** and **3d**.[16] The Rh−Si

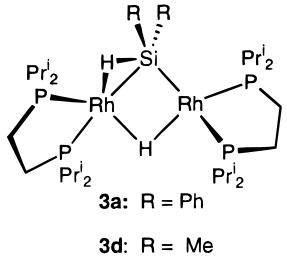

distances within the three-center, two-electron interactions are 0.20 and 0.13 Å longer than the corresponding unbridged Rh−Si bonds. In comparison to other dinuclear complexes with agostic Si−H bonds, these bond "lengthenings" represent oxidative additions of the Si−H bond to rhodium which have been arrested at an early and an intermediate stage, respectively.[25]

Complex **4d** is fluxional with an average structure in solution that is symmetric: all four phosphines are chemically equivalent, as are the four hydrides. When the temperature of a solution of **4d** is lowered and monitored by both $^{31}P\{^1H\}$ and ^1H NMR spectroscopy, decoalescence and spectra are observed that can be interpreted in terms of a slow exchange regime. A simple doublet observed at room temperature in the $^{31}P\{^1H\}$ NMR spectrum attests to the equivalence of the four phosphines (with coupling to ^{103}Rh) in the averaged structure. At approximately −29 °C a coalescence point is reached and at −54 °C two signals of equal intensity can be resolved. Thus, the process that exchanges two

(22) The coordinates for the molecular structure of **4d** were entered into the Chem 3D Plus program through a Molecule Editor using the Cache system by Techtronix, and the Si−Si distance was calculated using the Molecule Editor.

(23) Pham, E. K.; West, R. *Organometallics* **1990**, *9*, 1517.

(24) Zarate, E. A.; Tessier-Youngs, C. A.; Youngs, W. J. *J. Am. Chem. Soc.* **1988**, *110*, 4068.

(25) Schubert, U. *Adv. Organomet. Chem.* **1990**, *30*, 151.

pairs of phosphines between inequivalent sites in a less symmetric structure has been slowed on the NMR time scale at this temperature. A value for $\Delta G^{\ddagger}$(244 K) of 10.2 ± 0.2 kcal/mol was calculated for this process on the basis of the coalescence of the signals observed at −54 °C. Further cooling of **4d** to −94 °C causes four new signals to emerge in the $^{31}P\{^{1}H\}$ NMR spectrum, all broad doublets. The changes that occur in the spectra between −54 and −94 °C do not resemble a normal decoalescence and may be attributable to conformational effects of the various chelate rings in concert with the complicated core of the dinuclear complex. In the room-temperature ^{1}H NMR spectrum, a single hydride signal, a multiplet at −11.7 ppm, splits into two broad singlets as the sample is cooled to −64 °C, with coalescence occurring at −39 °C. This indicates that the two types of hydrides in the complex are being exchanged between inequivalent sites; the process responsible for this exchange has $\Delta G^{\ddagger}$(234 K) = 10.2 ± 0.2 kcal/mol, as calculated from the observed coalescence. Similar to what was seen in the $^{31}P\{^{1}H\}$ NMR spectra, when the sample is cooled to lower temperatures new signals emerge which appear to be due to four inequivalent hydrides in a less symmetric structure. Again, the changes in these spectra at low temperature are not typical of decoalescences but are more likely to be due to conformation effects.[26]

The coalescences observed in the above variabe-temperature NMR spectra are consistent with a fluxional process occurring for a solution structure that is approximately the same as the solid-state structure of **4d**. Two distinct phosphorus environments arise from

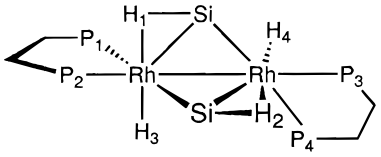

4d

(substituents at phosphorus and silicon have been omitted for clarity)

an orthogonal arrangement of the two chelate rings: one phosphine from each bis(phosphine) ligand (P_2, P_3) is *trans* to the Rh−Rh bond, and the two remaining phosphines (P_1, P_4) are each *trans* to an unbridged Rh−Si bond. P_1 and P_4 are chemically equivalent, as are P_2 and P_3, resulting in the two doublets observed in $^{31}P\{^{1}H\}$ NMR spectrum of **4d** at −54 °C. The strong *trans* influence of the silyl ligands in **4d**[27,28] allows us to assign the signals in this spectrum: empirical studies show that ^{31}P signals for phosphorus nuclei *trans* to strong *trans*-influence ligands are shifted to higher field, and

Scheme 2

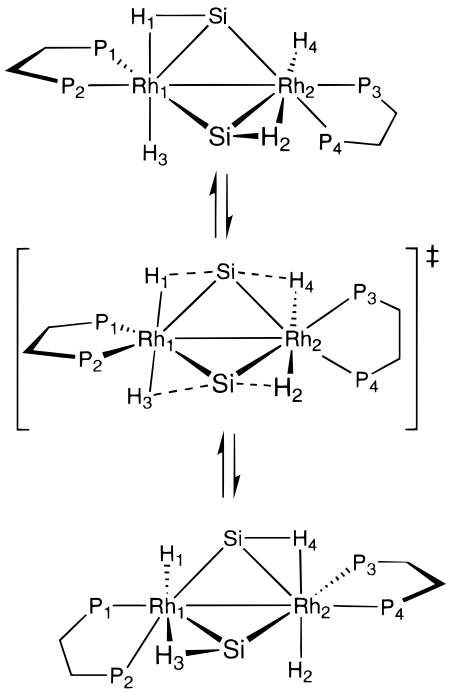

their J_{Rh-P} values tend to be significantly reduced.[29] Thus, the signal at 84 ppm ($^{1}J_{Rh-P}$ = 150 Hz) is due to the phosphines *trans* to Rh (P_2, P_3), whereas the signal at 72 ppm ($^{1}J_{Rh-P}$ = 97 Hz) is due to the phosphines *trans* to Si (P_1, P_4).

The hydride signals observed in the ^{1}H NMR spectrum at −64 °C are also consistent with the structure shown, where there are two types of hydride ligands: two are involved in the agostic Si−H bonds to rhodium (H_1 and H_2), and the others are terminal rhodium hydrides (H_3 and H_4).[30] Thus, the signal at −10.6 ppm is assigned to the agostic hydrides (H_1, H_2) and the signal at −12.7 ppm to the terminal hydrides (H_3, H_4).

A mechanism for exchange of phosphines and hydrides between inequivalent sites in **4d** is based on one previously established by variable-temperature NMR studies for a series of analogous bis(silyl) complexes derived from primary silanes (Scheme 2).[31] The mechanism involves simultaneous twisting of the two rhodium coordination spheres. At each rhodium center the H−Rh−H axis rotates through 90°, with concerted breaking of one agostic Si−H bond (*e.g.* Si−H_1) and the formation of another (*e.g.* Si−H_3): this process exchanges the terminal hydrides on rhodium and the agostic silicon hydrides. A concurrent twisting of the phosphine chelate rings through 90° exchanges the two types of phosphorus on each ligand (*e.g.* P_1, originally *trans* to silicon, becomes *trans* to Rh_2, while P_2 undergoes the opposite change).

The molecular structure of **4d** suggests that the complex should be extremely labile toward loss of either H_2 or Me_2SiH_2. The complex does decompose, particularly in solution at room temperature or above, to give

(26) The structure of this unsymmetrical species forming at low temperature in solutions of **4d** is not obvious. It may be a conformational isomer of the more symmetric structure corresponding to the low-temperature limit of the observed decoalescences, where the phosphine ligands, and hence the hydrides, are less symmetrically disposed.

(27) The strong *trans* influence of silyl ligands is manifested in the solid-state structure of **4d** in the lengthening of the Rh−P bond lengths by 0.1 Å for the phosphines (P_1, P_4) *trans* to the silyl ligands relative to the Rh−P bonds for the phosphines (P_2, P_3) *trans* to the Rh−Rh bond.

(28) Collman, J. P.; Hegedus, L. S.; Norton, J. R.; Finke, R. G. *Principles and Applications of Organotransition Metal Chemistry*; University Science Books: Mill Valley, CA, 1987; pp 242−243.

(29) Meek, D. W.; Mazanec, T. J. *Acc. Chem. Res.* **1981**, *14*, 266.

(30) It is possible that in solution the agostic Si−H bonds in **4d** have completely oxidatively added to give four terminal hydride ligands while the geometry of the complex remains approximately the same; this situation would still give rise to two types of hydride ligands.

(31) Fryzuk, M. D.; Rosenberg, L.; Rettig, S. J. *Inorg. Chim. Acta* **1994**, *222*, 345.

both $[(dippe)Rh]_2(\mu\text{-}SiMe_2)_2$ (**2d**) and **3d** (eq 4). The

$$\begin{array}{l}[(dippe)Rh(H)]_2(\mu\text{-}\eta^2\text{-}H\text{–}SiMe_2)_2 \\ \textbf{4d} \\ \quad\downarrow \Delta \\ [(dippe)Rh]_2(\mu\text{-}SiMe_2)_2 + 2H_2 + \\ \textbf{2d} \\ [(dippe)Rh]_2(\mu\text{-}H)(\mu\text{-}\eta^2\text{-}H\text{–}SiMe_2) + \\ \textbf{3d} \qquad\qquad Me_2SiH_2\end{array} \tag{4}$$

decomposition of **4d** can be directed toward one or the other of these products by careful control of the reaction conditions. When sealed NMR samples of **4d** are heated, the $^{31}P\{^1H\}$ NMR spectra show signals appearing for both **2d** and the hydrogen adduct of **3d**, $\{[(dippe)Rh]_2(\mu\text{-}H)(\mu\text{-}\eta^2\text{-}H{-}SiMe_2)\}\cdot H_2$.[21] However, when an NMR sample is heated at 45 °C while open to a nitrogen manifold and bubbler to allow any volatile products to escape the NMR tube, monitoring by $^{31}P\{^1H\}$ NMR shows the slow formation of a single product, **3d**. The positive pressure of nitrogen apparently discourages formation of the bis(μ-silylene) complex **2d**, and it may be that a slight vacuum, as is present in sealed NMR samples, is required to initiate the loss of hydrogen from **4d**. Alternatively, addition of ethylene to a solution of **4d** causes the quantitative formation of **2d** (eq 5). It is

$$\begin{array}{l}[(dippe)Rh(H)]_2(\mu\text{-}\eta^2\text{-}H\text{–}SiMe_2)_2 \\ \textbf{4d} \\ \quad\downarrow C_2H_4 \\ [(dippe)Rh]_2(\mu\text{-}SiMe_2)_2 + 2C_2H_6 \\ \textbf{2d} \\ \qquad (\text{or } + C_2H_4 + 2H_2)\end{array} \tag{5}$$

not clear whether the ethylene in this reaction is being hydrogenated by **4d**, or if the reversible coordination of ethylene simply prompts the elimination of hydrogen from the bis(silane) complex. A similar reaction was performed using styrene ($PhCH{=}CH_2$); however, this reaction did not proceed at room temperature, and heating the mixture caused decomposition of **4d** to **3d** and **2d**. No ethylbenzene was detected. Complex **4d** may be regenerated by placing solutions of **2d** under an atmosphere of hydrogen.

Placing a solution of **4d** under an atmosphere of dihydrogen leaves the molecule apparently unchanged, as shown by $^{31}P\{^1H\}$ NMR spectroscopy. However, there is evidence for a slow exchange: NMR spectroscopic monitoring of a sample of **4d** sealed under deuterium gas by ^1H NMR spectroscopy showed a slow decrease in intensity of the hydride resonance relative to the ligand resonances in the spectra.

Formation of the bis(μ-silylene) complexes **2a**–**c** probably proceeds via the initial bis(silane) adduct **II**, which is analogous to **4d**. As in the decomposition of **4d** to **2d** described above, elimination of 2 equiv of H_2 from an intermediate such as **II** would generate a bis(μ-silylene) complex; the formation of such an intermediate has already been directly observed by monitoring the reactions of primary silanes with **1**.[31] The butterfly-shaped core of the proposed intermediates **4a**–**c** would be sterically hindered relative to **4d**; these higher energy

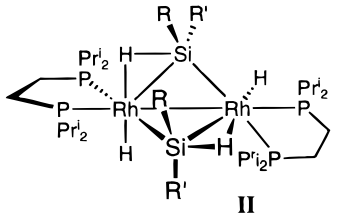

II

4a: R = R' = Ph
4b: R = Me, R' = Ph
4c: R = Me, R' = Tol^p

species have not been isolated or detected spectroscopically. While for **4d** no elimination of a Si–Si-bonded species was observed under any of these reaction conditions, the increased crowding at proposed intermediate **4a** might facilitate Si–Si reductive coupling.[32]

Catalytic Dimerization of Diphenylsilane. We previously reported the catalytic activity of **1** in the isotopic exchange of hydrides for deuterides on diphenylsilane, with deuterium gas as a source of deuterides (eq 6).[14] Higher substrate concentrations and the use

$$Ph_2SiH_2 \xrightarrow[\text{1 atm}\\ \text{RT}]{D_2,\ [(dippe)Rh]_2(\mu\text{-}H)_2} Ph_2SiD_2 \tag{6}$$

of aromatic solvents appear to encourage a side reaction, the disproportionation of diphenylsilane to triphenylsilane and phenylsilane (eq 7), though monitoring the

$$2\ Ph_2SiH_2 \xrightarrow[\text{RT}]{[(dippe)Rh]_2(\mu\text{-}H)_2} Ph_3SiH + PhSiH_3 \tag{7}$$

reaction in d_6-benzene by ^1H NMR spectroscopy indicates that the deuterium exchange reaction occurs more quickly than the disproportionation reaction.[11,21,33] Very high concentrations of diphenylsilane, or the addition of the catalyst to the diphenylsilane *prior* to the introduction of deuterium, tends to give small amounts of 1,1,2,2-tetraphenyldisilane, the product of dehydrogenative dimerization of diphenylsilane (eq 8). When the

$$2\ Ph_2SiH_2 \xrightarrow[\text{RT}\\ (-H_2)]{[(dippe)Rh]_2(\mu\text{-}H)_2} Ph_2HSi\text{–}SiHPh_2 \tag{8}$$

deuterium atmosphere is replaced by nitrogen, dimerization of diphenylsilane becomes the major process occurring in the presence of catalytic amounts of **1**.[14]

The active species in the dimerization of diphenylsilane as catalyzed by **1** may be dinuclear rather than

(32) The recently reported structure of a dicobalt complex, constrained to a butterfly-shaped core by the bridging disilyl ligand –Si(Me)CH_2CH_2Si(Me)–, shows an extremely short Si···Si separation of 2.691(2) Å. It is suggested that optimization of the Co–Si bonding in this type of structure forces the reduction of the Si–Co–Si angles, due to overlap of filled Co d orbitals with empty σ^* orbitals located mainly on the Si's: Bourg, S.; Boury, B.; Carré, F.; Corriu, R. J. P. *Organometallics* **1997**, *16*, 3097. Similarly, a short Si···Si separation of 2.85 Å was reported for a dinuclear rhodium complex with bridging silicons where a "cradle" structure approaches the same geometry as observed for **4d**: Wang, W.-D.; Eisenberg, R. *J. Am. Chem. Soc.* **1990**, *112*, 2, 1833.

(33) The disproportionation of organosilicon compounds in the presence of transition metals, requiring activation of both Si–H and Si–C bonds, is quite common, though not well-understood.

Scheme 3

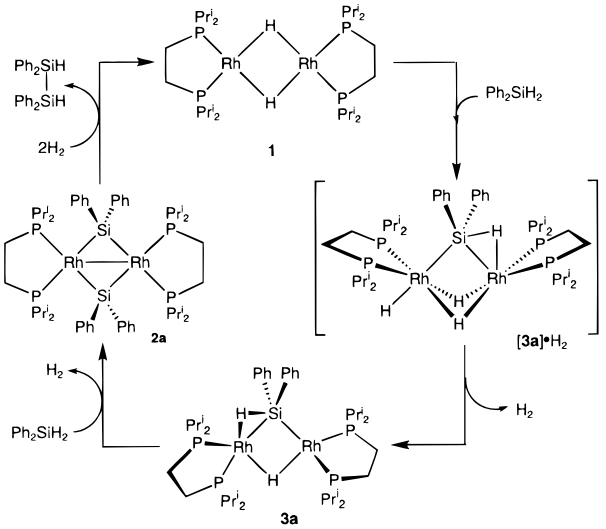

Scheme 4

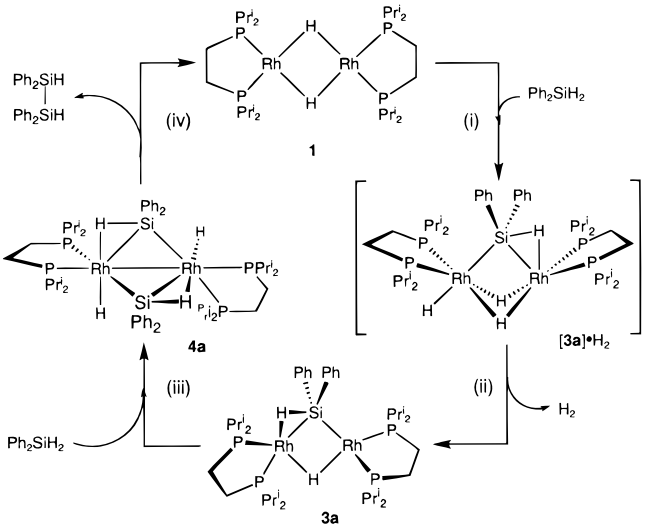

mononuclear. Scheme 3 shows a possible catalytic cycle, based on the same progression of oxidative-addition and reductive-elimination steps as depicted in Scheme 1: all of these reactions occur at dinuclear centers and generate dinuclear products, and all of the complexes shown have been isolated or identified spectroscopically.

To establish the activity of **2a** in this dehydrogenative coupling reaction, we examined its reactivity with diphenylsilane, in the absence of complexes **1** and **3a**. In the presence of excess diphenylsilane (4−5 equiv) an orange solution of **2a** in benzene reacts to give a yellow solution. The $^{31}P\{^{1}H\}$ NMR spectrum of this solution is complex but may be attributed to a single complex in solution, compound **5**. The ^{1}H NMR spectrum of the reaction mixture indicates the presence of both rhodium hydrides and terminal silicon hydrides in **5** and also the presence of triphenylsilane and unreacted diphenylsilane. Phenylsilane, the byproduct of the disproportionation reaction that produces triphenylsilane, is not observed. It is possible that **5** results from the reaction of **2a** with $PhSiH_3$ and is a "mixed silane" analogue of tris(silyl) complexes previously isolated from the reactions of *n*-butylsilane and *p*-tolylsilane with **1**.[31] Complex **5** has not been isolated pure in the solid state. No tetraphenyldisilane was observed in the reaction mixture; therefore **2a** is *not* responsible for the catalytic silicon coupling reaction observed in the presence of **1** and diphenylsilane. This is consistent with our earlier observation that **2a** does not react with hydrogen to give **1**.

Scheme 4 shows a more likely catalytic cycle, invoking the activity of proposed intermediate **4a** in the silicon−silicon coupling reaction. As discussed above, **4a** is strongly implicated as an intermediate in the formation of **2a**. This complex should be extremely reactive (as evidenced by the solution behavior of its dimethylsilane analogue **4d**) and prone to reductive elimination of a silicon−silicon bond (*vide supra*). Thus, in the stoichiometric chemistry of this system described so far, there is evidence of (i) oxidative addition of silane to a metal hydride complex with (ii) elimination of hydrogen to generate a silyl complex[16] and (iii) oxidative addition of silane to a metal silyl complex.[31]

Step iv in the catalytic cycle shown in Scheme 4, the reductive elimination of a Si−Si bond, has not been directly observed for the dinuclear rhodium center of this system. However, the reverse reaction, oxidative addition of a Si−Si bond to **1**, does occur stoichiometrically. When a mixture of 1,1,2,2-tetraphenyldisilane and **1** in toluene is heated to 70 °C, the major product observed by $^{31}P\{^{1}H\}$ NMR is **3a**, the formation of which requires the cleavage of the Si−Si bond of the disilane (eq 9). Thus the transition state or intermediate required for a Si−Si bond-breaking step is thermodynamically accessible for this dinuclear system; presumably that for the Si−Si bond formation step must also be accessible. The principal silicon-containing compound in this reaction mixture is unreacted disilane. Scheme 5 outlines the various equilibria involved in this reaction, *assuming that the initial adduct of the disilane with* **1** *is intermediate* **4a**, with a structure analogous to **4d** (step A). This intermediate has already been identified as a likely precursor for the reductive elimination of a silicon−silicon bond from the dinuclear rhodium center (*vide supra*) and, like **4d**, would also be capable of decomposing through elimination of either hydrogen (step B) or silane (step C). However, in the presence of equilibrium amounts of **1**, any diphenylsilane formed reacts instantly and irreversibly to give **3a** plus hydrogen (step D). This reaction consumes **1**, shifting the initial equilibrium (A) to the left. The irreversibility of step D in this system is ultimately responsible for the final product mixture of **3a** and 1,1,2,2-tetraphenyldisilane. Hydrogen is also being eliminated from **4a** to give **2a** (B), but in the presence of hydrogen (generated by the reaction of **1** with diphenylsilane; step D) this reaction is easily reversed, particularly at high temperatures.

$$\underset{\mathbf{1}}{[(\text{dippe})\text{Rh}]_2(\mu\text{-H})_2} + \text{Ph}_2\text{SiH–HSiPh}_2 \xrightarrow[\text{toluene}]{70^\circ\text{C}} \underset{\mathbf{3a}}{[(\text{dippe})\text{Rh}]_2(\mu\text{-H})(\mu\text{-}\eta^2\text{-H–SiPh}_2)} + \tfrac{1}{2}\,\text{Ph}_2\text{SiH–HSiPh}_2 + \tfrac{1}{2}\,\text{H}_2 \quad (9)$$

Scheme 5

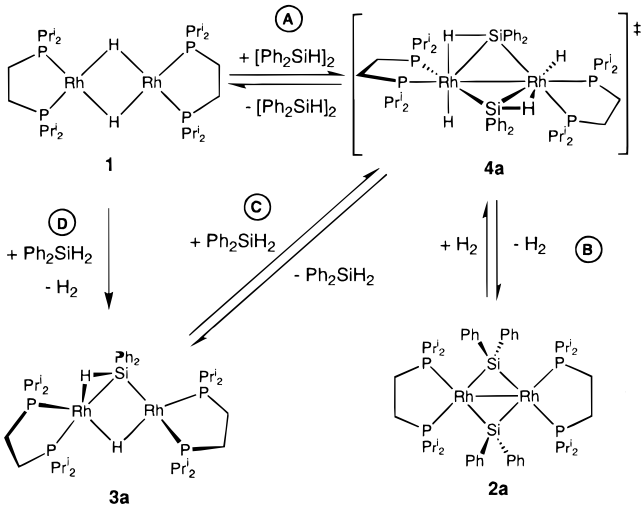

It is important to note that, for the reaction shown in eq 9, the observed results require *the formation of an intermediate* **4a** *from* **1** *and 1,1,2,2-tetraphenyldisilane* and also require that its *formation be reversible.* This implied reversibility is the key to the catalytic activity of **4a**: we propose that complex **4a** represents the final intermediate in the catalytic dehydrogenative coupling of diphenylsilane to give 1,1,2,2-tetraphenyldisilane.

Experimental Section

General Procedures and Reagent Syntheses. All manipulations were performed under prepurified nitrogen in a Vacuum Atmospheres HE-553-2 workstation equipped with an MO-40-2H purification system or using Schlenk-type glassware. The term "reactor bomb" refers to a cylindrical, thick-walled Pyrex vessel equipped with a 5 mm (or 10 mm, for larger bombs) Kontes Teflon needle valve and a ground-glass joint for attachment to a vacuum line. NMR tubes used for preparing sealed samples are 8 or 9 in. Wilmad 507 PP NMR tubes with an outer b14 joint attached by glass-blowing.

Toluene and hexanes were predried over CaH_2 and then distilled from molten sodium and sodium−benzophenone ketyl, respectively, under argon. Deuterated benzene (C_6D_6, 99.6 atom % D) and deuterated toluene (C_7D_8, 99.6 atom % D) were purchased from MSD Isotopes and dried over 4 Å molecular sieves. The dried deuterated solvents were then degassed using three "freeze−pump−thaw" cycles and were vacuum-transferred before use. Ethylene and deuterium gas were purchased from Matheson Gas Products, the deuterium being passed through a glass coil immersed in liquid nitrogen to remove any traces of water and oxygen. Hydrogen gas was purified by being passed through a column packed with activated 4 Å molecular sieves and MnO.

Literature methods were used to prepare [(dippe)Rh]$_2$(μ-H)$_2$ (**1**).[17,34] Ph_2SiH_2 and $MePhSiH_2$ were purchased from the Aldrich Chemical Co., dried by refluxing over calcium hydride overnight, and distilled. The silanes Me_2SiH_2 and $MeTol^pSiH_2$ were prepared by $LiAlH_4$ reduction of Me_2SiCl_2 (purchased from Aldrich) and $MeTol^pSiCl_2$ (purchased from Petrarch Systems) using slightly modified literature procedures.[21,35,36]

^{1}H NMR spectra were recorded on Varian XL-300, Bruker WP-200, Bruker WH-400, and Bruker AMX-500 spectrometers. With d_6-benzene as solvent the spectra were referenced to C_6D_5H at 7.15 ppm and with d_8-toluene as solvent the spectra were referenced to the CD_2H residual proton at 2.09 ppm. ^{31}P-{^{1}H} NMR spectra were recorded at 121.4 MHz on the Varian XL-300 or at 202.3 MHz on the Bruker AMX-500 and were referenced to external $P(OMe)_3$ at +141.0 ppm relative to 85% H_3PO_4. ^{29}Si NMR spectra were run at 59.6 MHz on the Varian XL-300 and were referenced to external TMS at 0.0 ppm.

Elemental analyses were carried out by Mr. P. Borda of this department. Gas chromatography/mass spectrometry was carried out by Ms. L. Madilao of this department.

Syntheses of Complexes and Reactivity Studies. [(dippe)Rh]$_2$(μ-H)(μ-η^2-H−SiMeTol^p) (3c). This complex was prepared by the same method as for **3a**,**b**,**d** (113 mg (0.154 mmol) of **1**; 21 mg (0.154 mmol) of methyl-*p*-tolylsilane).[16] Reddish brown crystals were obtained in 76% yield (102 mg). ^{1}H NMR (C_6D_6, ppm): H_{ortho} 7.93 (d, 2H, $^3J_{H_m-H_o}$ = 7.3 Hz); H_{meta} 7.13 (d, 2H); $SiC_6H_5CH_3$ 2.17 (s, 3H); $CH(CH_3)_2$ 1.98 (mult, 8H); PCH_2CH_2P, $SiCH_3$ 1.26−1.36 (overlapping d and s, 11H); $CH(CH_3)_2$ 1.21 (dd, 12H, $^3J_{P-H}$ = 14.5 Hz, $^3J_{H-H}$ = 7.0 Hz); $CH(CH_3)_2$ 1.12−0.94 (mult, 36H); Rh−*H* −6.00 (pt, 2H, J_{P-H} = 20.6 Hz, $^1J_{Rh-H}$ = 15.7 Hz). Note: For **3c** in d_8-toluene the singlet resonance due to $SiCH_3$ shifts to 1.24 ppm and the PCH_2CH_2P resonance is seen as a doublet at 1.33 ppm ($^2J_{P-H}$ = 12.6 Hz). ^{31}P{^{1}H} NMR (C_6D_6, ppm): 94.3 (d mult, J_{Rh-P} = 159 Hz). ^{29}Si NMR (C_7D_8, ppm): 157−166 (br mult). Anal. Calcd for $C_{36}H_{76}P_4Rh_2Si$: C, 49.88; H, 8.84. Found: C, 50.20; H, 8.86.

[(dippe)Rh]$_2$(μ-SiPh$_2$)$_2$ (2a). This compound can be prepared by two methods.

(1) To a red solution of [(dippe)Rh]$_2$(μ-H)(μ-η^2-H−SiPh$_2$) (**3a**;[16] 275 mg, 0.300 mmol) in hexanes (5 mL) was added dropwise a solution of diphenylsilane (55 mg, 0.300 mmol) in hexanes (3 mL). The supernatant was decanted from the bright yellow-orange precipitate that formed, and the precipitate was washed with cold hexanes to remove any unreacted silyl hydride complex. The yellow solid was then stirred in a large volume of toluene (25−30 mL) for several days until most of the powder had dissolved to give a bright orange solution. After filtration of the solution through a Celite pad, orange crystals were obtained from a minimum volume of toluene by cooling to −40 °C. Yield: 58% (191 mg).

(2) A reaction identical with that described above was carried out in toluene instead of hexanes. The dark red solution of **3a** changed to bright orange upon addition of the diphenylsilane. After filtration of the solution through a Celite pad, orange crystals were obtained from a minimum volume of toluene by cooling to −40 °C.

While the second method described is faster and more straightforward, it tends to give lower yields and second crops can be contaminated with any excess **3a** left in solution. The identity of the yellow powder formed from the first method has not yet been established.

^{1}H NMR (C_6D_6, ppm): H_{ortho} 8.31 (dd, 4H, $^3J_{H_m-H_o}$ = 7.2 Hz, $^4J_{H_p-H_o}$ = 1.3 Hz); H_{meta}, H_{para} 7.38−7.20 (overlapping mults, 6H); $CH(CH_3)_2$ 1.96 (mult, 8H); PCH_2CH_2P 1.30 (d, 8H, $^2J_{P-H}$ = 15.2 Hz), $CH(CH_3)_2$, 0.97−0.74 (mult, 48H). ^{31}P{^{1}H} NMR (C_6D_6, ppm): 79.3 (d mult, J_{Rh-P} = 134 Hz). Anal. Calcd for $C_{52}H_{84}P_4Rh_2Si_2$: C, 57.03; H, 7.73. Found: C, 56.79; H, 7.72.

Reaction of [(dippe)Rh]$_2$(μ-SiPh$_2$)$_2$ (2a) with H$_2$. This reaction was carried out on a larger scale, as described previously for the preparation of d_2-**3a** from **2a** and deuterium gas,[16] with diphenylsilane being identified by ^{1}H NMR spectroscopy as the principal organosilicon product. The reaction was also carried out in a sealed NMR tube and monitored over several days: [(dippe)Rh]$_2$(μ-SiPh$_2$)$_2$ (**2a**; 25 mg, 0.023 mmol) was dissolved in d_8-toluene (0.6 mL) in a sealable NMR tube. The solution was degassed by one freeze−pump−thaw cycle. One atmosphere of hydrogen gas was introduced, and the

(34) Fryzuk, M. D.; McConville, D. H.; Rettig, S. J. *J. Organomet. Chem.* **1993**, *445*, 245.

(35) Doyle, M. P.; DeBruyn, D. J.; Donnelly, S. J.; Kooistra, D. A.; Odubela, A. A.; West, C. T.; Zonnebelt, S. M. *J. Org. Chem.* **1974**, *39*, 2740.

(36) Benkeser, R. A.; Landesman, H.; Foster, D. J. *J. Am. Chem. Soc.* **1952**, *74*, 648.

sample was sealed. The sample was then frozen in liquid nitrogen while being transported to the NMR spectrometer and then thawed (the orange solution did not change in color) and placed in the spectrometer. The initial ^{1}H NMR spectrum showed signals due to the starting bis(μ-silylene) species **2a**, [[(dippe)Rh]$_2$(μ-H)(μ-η²-H−SiPh$_2$)]·H$_2$ (**3a**·H$_2$),[21] Ph$_2$SiH$_2$, and an unknown species (H$_{ortho}$ at 8.15 ppm). The initial ^{31}P{^{1}H} NMR spectrum showed signals due to **2a** and [[(dippe)Rh]$_2$-(μ-H)(μ-η²-H−SiPh$_2$)]·H$_2$ and also peaks due to a minor product at 90 ppm (br d) and at 78.8 ppm (d). The spectra were run again after the sample had sat at room temperature for 2 days. The ^{31}P{^{1}H} NMR spectrum showed the presence of only two products, **3a** and an as-yet unidentified complex, **5**, which is thought to result from the reaction of **2a** with the product of disproportionation of diphenylsilane, PhSiH$_3$ (see the following reaction). This is further supported by the ^{1}H NMR spectrum, which shows the presence of both Ph$_2$SiH$_2$ and Ph$_3$SiH, along with a signal (overlapping with that due to dissolved hydrogen) that might be due to [PhSiH$_2$]$_2$.

Reaction of [(dippe)Rh]$_2$(μ-SiPh$_2$)$_2$ (2a) with Excess Ph$_2$SiH$_2$. A solution of [(dippe)Rh]$_2$(μ-SiPh$_2$)$_2$ (**2a**; 10 mg, 0.0091 mmol) in d_6-benzene was added to diphenylsilane (7 mg, 0.037 mmol). Over 1 day the solution color changed from bright orange to yellow. ^{31}P{^{1}H} NMR spectroscopy showed the presence of a single product, complex **5**. Signals due to **5** as well as Ph$_2$SiH$_2$ and Ph$_3$SiH were observed in the ^{1}H NMR spectrum, along with an unassigned signal at 5.93 ppm.

Complex **5** was never isolated free of silicon-containing byproducts; therefore some of the peaks in the aromatic region were buried under peaks due to the other products, and relative integrals for the aromatic protons were unobtainable. Relative integrals and peak assignments are tentative. ^{1}H NMR (C$_6$D$_6$, ppm): Si−*H* 8.56 (br s, 2H, $w_{1/2}$ = 30 Hz); H$_{ortho}$ 8.27 (d, $^3J_{H_m-H_o}$ = 6.9 Hz); H$_{ortho}$ 8.04 (dd, $^3J_{H_m-H_o}$ = 7.6 Hz, $^3J_{H_p-H_o}$ = 1.6 Hz); H$_{meta}$ 7.44 (mult); C*H*(CH$_3$)$_2$ 2.54 (mult, 4H); C*H*(CH$_3$)$_2$ 2.11 (mult, 4H); CH(C*H*$_3$)$_2$, 1.65 (dd, 12H, $^3J_{P-H}$ = 13.5 Hz, $^3J_{H-H}$ = 7.2 Hz); PC*H*$_2$C*H*$_2$P, CH(C*H*$_3$)$_2$ 1.52−0.49 (overlapping mult, 32H); CH(C*H*$_3$)$_2$, 0.25 (dd, 12H, $^3J_{P-H}$ = 15.6 Hz, $^3J_{H-H}$ = 7.2 Hz); Rh−*H* −4.46 (br s, 2H, $w_{1/2}$ = 55 Hz); Rh−*H* −6.79 (br s, 1H, $w_{1/2}$ = 60 Hz); Rh−*H* −13.05 (br s, 1H, $w_{1/2}$ = 25 Hz); Rh−*H* −13.48 (br s, 1H, $w_{1/2}$ = 25 Hz). ^{31}P{^{1}H} NMR (C$_6$D$_6$, ppm): 98.1 (d mult, 1P); 85.1 (d mult, 1P); 82.9 (d mult, 1P); 72.4 (mult, 1P).

[(dippe)Rh]$_2$(μ-SiMePh)$_2$ (2b). This complex can be prepared by the same methods as for **2a** (96 mg (0.113 mmol) of **3d**; 14 mg (0.113 mmol) of MePhSiH$_2$; yield 65% (72 mg)). Unfortunately, even when the reaction is carried out in toluene the product tends to precipitate quickly, giving a bright orange powder which has low solubility in most common solvents. However, slow evaporation of a very dilute hexanes solution did eventually yield crystals suitable for an X-ray crystallographic study. This complex has two geometric isomers, *cis* and *trans*, which could not be completely separated by crystallization, despite the fact that the *trans* isomer is less soluble than the *cis* isomer.

trans-**2b**. ^{1}H NMR (C$_6$D$_6$, ppm): H$_{ortho}$ 7.71 (dd, 4H, $^3J_{H_m-H_o}$ = 6.6 Hz, $^4J_{H_p-H_o}$ = 1.5 Hz); H$_{meta}$ 7.17 (mult, 4H); H$_{para}$ 7.08 (mult, 2H); C*H*(CH$_3$)$_2$ 2.38 (mult, 8H); SiC*H*$_3$ 1.71 (s, 6H); PC*H*$_2$C*H*$_2$P 1.64−1.47 (mult, 4H); CH(C*H*$_3$)$_2$ 1.19 (dd, 12H, $^3J_{P-H}$ = 17.1 Hz, $^3J_{H-H}$ = 7.2 Hz); PC*H*$_2$C*H*$_2$P, CH(C*H*$_3$)$_2$ 1.14−0.92 (mult, 28H); CH(C*H*$_3$)$_2$ 0.53 (dd, 12H, $^3J_{P-H}$ = 15.6 Hz, $^3J_{H-H}$ = 7.3 Hz). ^{31}P{^{1}H} NMR (C$_6$D$_6$, ppm): 82.8 (d mult, $^1J_{Rh-P}$ = 162 Hz).

cis-**2b**. ^{1}H NMR (C$_6$D$_6$, ppm): H$_{ortho}$ 8.03 (dd, 4H, $^3J_{H_m-H_o}$ = 7.8 Hz, $^4J_{H_p-H_o}$ = 1.2 Hz); H$_{meta}$ 7.33 (t, 4H, J_{avg} = 7.2 Hz); H$_{para}$ 7.19 (mult, 2H); C*H*(CH$_3$)$_2$ 2.27 (br s, 4H); C*H*(CH$_3$)$_2$ 2.06 (br s, 4H); SiC*H*$_3$, PC*H*$_2$C*H*$_2$P 1.43−1.30 (overlapping s and d, 14H); CH(C*H*$_3$)$_2$ 1.17−0.91 (mult, 48H). ^{31}P{^{1}H} NMR (C$_6$D$_6$, ppm): 80.9 (d mult, $^1J_{Rh-P}$ = 163 Hz).

Anal. Calcd for C$_{42}$H$_{80}$P$_4$Rh$_2$Si$_2$·0.3C$_7$H$_8$: C, 52.85; H, 8.29. Found: C, 52.84; H, 8.30.

[(dippe)Rh]$_2$(μ-SiMeTol^p)$_2$ (2c). To a stirred, dark green solution of [(dippe)Rh]$_2$(μ-H)$_2$ (**1**; 107 mg, 0.146 mmol) in hexanes (5 mL) was added dropwise a solution of methyl-*p*-tolylsilane (40 mg, 0.292 mmol) in hexanes (10 mL) to give a bright orange solution. After filtration of the solution through a Celite pad, orange crystals were obtained from a minimum volume of hexanes by cooling to −40 °C. Yield: 71% (104 mg). While both *cis* and *trans* isomers are formed from this reaction, the less soluble *trans* isomer can be isolated by fractional crystallization. This complex can also be prepared from the addition of a single equivalent of methyl-*p*-tolylsilane to **3c**.

trans-**2c**. ^{1}H NMR (C$_6$D$_6$, ppm): H$_{ortho}$ 7.64 (d, 4H, $^3J_{H_o-H_m}$ = 7.5 Hz); H$_{meta}$ 7.03 (d, 4H), C*H*(CH$_3$)$_2$ 2.50−2.29 (overlapping mult, 8H); SiC$_6$H$_5$C*H*$_3$ 2.13 (s, 6H); SiC*H*$_3$ 1.73 (br s, 6H); PC*H*$_2$C*H*$_2$P 1.63−1.45 (mult, 4H); CH(C*H*$_3$)$_2$ 1.22 (dd, 12H, $^3J_{H-P}$ = 18.3 Hz, $^3J_{H-H}$ = 7.5 Hz); PC*H*$_2$C*H*$_2$P, CH(C*H*$_3$)$_2$ 1.13−0.94 (mult, 28H); CH(C*H*$_3$)$_2$ 0.57 (dd, 12H, $^3J_{H-P}$ = 15.3 Hz, $^3J_{H-H}$ = 7.2 Hz). ^{31}P{^{1}H} NMR (C$_6$D$_6$, ppm): 82.7 (d mult, J_{P-Rh} = 161 Hz).

cis-**2c**. ^{1}H NMR (C$_7$D$_8$, ppm): H$_{ortho}$ 7.86 (d, 4H, $^3J_{H_o-H_m}$ = 7.8 Hz); H$_{meta}$ 7.11 (d, 4H); C*H*(CH$_3$)$_2$ 2.37−1.92 (overlapping mult, 8H); SiC$_6$H$_5$C*H*$_3$ 2.19 (s, 6H); PC*H*$_2$C*H*$_2$P, SiC*H*$_3$ 1.38−1.27 (overlapping s and d, 14H); CH(C*H*$_3$)$_2$ 1.15−0.85 (mult, 48H). ^{31}P{^{1}H} NMR (C$_6$D$_6$, ppm): 80.8 (d mult, J_{P-Rh} = 163 Hz).

Anal. Calcd for C$_{44}$H$_{84}$P$_4$Rh$_2$Si$_2$: C, 52.90; H, 8.47. Found: C, 52.66; H, 8.40.

Conversion of Pure *trans*-2c to *cis/trans* Mixtures. A solution of *trans*-[(dippe)Rh]$_2$(μ-SiMeTol^p)$_2$ (**2c**; 23 mg, 0.023 mmol) in d_8-toluene (0.6 mL) was placed in an NMR tube with a Teflon screw cap. The tube was closed and heated to the appropriate temperature (70, 90, 110, or 130 °C) in an oil bath. The tube was removed from the oil bath once every 30 min and was placed in an ice bath to quench the equilibration reaction. A ^{1}H NMR spectrum of the sample was run before returning the sample to the oil bath. Appearance of the *cis* isomer in solution was monitored by integration of the H$_{ortho}$ signals at 7.64 ppm (*trans*) and 7.86 ppm (*cis*). The samples were heated over 8−10 h periods.

[(dippe)Rh(H)]$_2$(μ-η²-H−SiMe$_2$)$_2$ (4d). Dimethylsilane (0.840 mmol, 2.1 equiv, 271 mmHg in a 57.5 mL constant-volume bulb) was vacuum-transferred to a dark green solution of [(dippe)Rh]$_2$(μ-H)$_2$ (**1**; 293 mg, 0.400 mmol) in frozen hexanes (5 mL) at −196 °C. The solution was warmed slightly below room temperature (ice−water bath), by which time the solution had changed to a pale, golden yellow color. Yellow crystals were obtained from a minimum volume of hexanes by cooling to −40 °C. Yield: 62% (211 mg). The product is obtained in purest form if a minimum of hexanes is used from the start of the reaction and if the solution is kept cool throughout. If solvent has to be removed from the product solution to induce crystallization, there is normally some decomposition of the product to [(dippe)Rh]$_2$(μ-H)(μ-η²-H−SiMe$_2$) (**3d**)[16] and [(dippe)-Rh]$_2$(μ-SiMe$_2$)$_2$ (**2d**); i.e.. loss of 1 equiv of silane or 1 equiv of hydrogen. This same decomposition occurs slowly if solutions of **4d** are allowed to stand at room temperature for periods of time longer than 5−10 min. Complex **4d** can also be prepared by the addition by vacuum transfer of 1 equiv of dimethylsilane to a solution of **3d** in hexanes, with similar yields. ^{1}H NMR (C$_7$D$_8$, ppm): C*H*(CH$_3$)$_2$ 1.91 (mult, 8H, $^3J_{H-H}$ = 7.0 Hz); PC*H*$_2$C*H*$_2$P 1.25 (d, 8H, $^2J_{P-H}$ = 10.4 Hz); CH(C*H*$_3$)$_2$ 1.16−1.02 (two dd); Si(C*H*$_3$)$_2$ 0.88 (s, 12H); Rh−*H* −11.59 (mult (second-order pattern), 4H). Note: In d_6-benzene the Si(C*H*$_3$)$_2$ resonance is seen as two singlets at 0.94 and 0.98 ppm; it is not known why the two inequivalent signals arise. **^{31}P{^{1}H} NMR** (C$_6$D$_6$, ppm): 77.3 (br d, J_{Rh-P} = 118 Hz). Anal. Calcd for C$_{32}$H$_{80}$P$_4$Rh$_2$Si$_2$: C, 45.17; H, 9.48. Found: C, 45.30; H, 9.60.

Thermal Decomposition of [(dippe)Rh(H)]$_2$(μ-η²-H−SiMe$_2$)$_2$ (4d). Approximately 25 mg (0.029 mmol) of [(dippe)-Rh(H)]$_2$(μ-η²-H-SiMe$_2$)$_2$ (**4d**) was dissolved in d_8-toluene in an NMR tube equipped with a Teflon screw cap/gas inlet adapter.

An initial $^{31}P\{^1H\}$ NMR spectrum was run to establish the purity of the sample; then the sample was attached to a nitrogen manifold. The sample was heated in an oil bath at 45 °C while open to the nitrogen manifold and bubbler, to allow any volatile products to escape the NMR tube. The progress of the reaction was checked periodically by $^{31}P\{^1H\}$ NMR spectroscopy. After 4 h a substantial amount of $[(dippe)Rh]_2(\mu\text{-H})(\mu\text{-}\eta^2\text{-H}-SiMe_2)$ (**3d**) had formed, with 23% conversion of **4d** to **3d**. After 24 h all of **4d** had disappeared, giving **3d** as the principal product, along with some decomposition products due to traces of air and water in the system.

Reaction of $[(dippe)Rh(H)]_2(\mu\text{-}\eta^2\text{-H}-SiMe_2)_2$ (4d) with H_2. Approximately 25 mg (0.029 mmol) of $[(dippe)Rh(H)]_2(\mu\text{-}\eta^2\text{-H-}SiMe_2)_2$ (**4d**) was dissolved in d_8-toluene in a sealable NMR tube. The tube was attached to a vacuum line by a needle valve adapter, and slightly less than 1 atm of hydrogen was introduced. No color change was observed. The ^1H and $^{31}P\{^1H\}$ NMR spectra of the sealed sample revealed that no reaction with the hydrogen had occurred. In the ^1H NMR spectrum the hydride resonance at −11.59 ppm had lost resolution, which might indicate that hydride exchange with hydrogen in solution was occurring.

Reaction of $[(dippe)Rh(H)]_2(\mu\text{-}\eta^2\text{-H}-SiMe_2)_2$ (4d) with D_2. This reaction was carried out in the same manner as the preceding reaction, except that the sealable NMR tube containing solid **4d** was cooled in an ice bath before the addition of the d_8-toluene and the solution was kept cool while the deuterium gas was added and the tube was sealed. The initial $^{31}P\{^1H\}$ and ^1H NMR spectra showed no reaction with the deuterium. The sample was monitored by NMR spectroscopy over a 2-week period, after which time approximately 50% of the hydride in the sample had been exchanged for deuteride, as determined from integration of the ^1H NMR spectrum.

$[(dippe)Rh]_2(\mu\text{-}SiMe_2)_2$ (2d). This complex is formed by dissociation of 2 equiv of H_2 from **4d** if it is left in solution at room temperature or is heated. However, it is difficult to get complete conversion to **2d** by this method; the product is often mixed with leftover **4d** and with **3d** formed by a concurrent dissociation of dimethylsilane. A reaction which gives pure **2d** as product is that of **4d** with an excess of ethylene. Solid $[(dippe)Rh(H)]_2(\mu\text{-}\eta^2\text{-H}-SiMe_2)_2$ (**4d**; 58 mg, 0.068 mmol) was weighed into a thick-walled reactor bomb. The bomb was cooled to 0 °C in an ice bath, and under a strong flow of nitrogen, toluene (5 mL) was added, giving a pale, golden yellow solution. The headspace above the solution was evacuated, and 1 atm of ethylene was introduced. The solution was stirred at 0 °C for 15 min, during which time the solution color changed to orange-red. Orange-red crystals were obtained from a minimum volume of toluene by cooling to −40 °C. Yield: 68% (39 mg). ^1H NMR (C_6D_6, ppm): $CH(CH_3)_2$ 2.18 (mult, 8H); PCH_2CH_2P 1.36 (d, 8H, $^2J_{P-H} = 15.3$ Hz); $Si(CH_3)_2$ 1.14 (s, 12H) overlapping with $CH(CH_3)_2$ 1.18−1.02 (overlapping mult, 48H). Note: For **2d** in d_8-toluene the $Si(CH_3)_2$ resonance is seen at 1.04 ppm, a solvent-related, upfield shift of 0.10 ppm. $^{31}P\{^1H\}$ NMR (C_6D_6, ppm): 83.3 (d mult, $^1J_{Rh-P} = 167$ Hz). Anal. Calcd for $C_{32}H_{80}P_4Rh_2Si_2$: C, 45.17; H, 9.48. Found: C, 45.30; H, 9.60.

Reaction of $[(dippe)Rh]_2(\mu\text{-}SiMe_2)_2$ (2d) with H_2. Approximately 25 mg (0.030 mmol) of $[(dippe)Rh]_2(\mu\text{-}SiMe_2)_2$ (**2d**) was dissolved in d_8-toluene in a sealable NMR tube. The tube was attached to a vacuum line by a needle valve adapter, and slightly less than 1 atm of hydrogen was introduced. The tube was tapped for 5−10 min to encourage diffusion of the gas into the orange-red solution, which changed to a pale yellow color. The tube was sealed, and NMR spectra (^1H and $^{31}P\{^1H\}$) of the sample were run. The product of the reaction was $[(dippe)Rh(H)]_2(\mu\text{-}\eta^2\text{-H}-SiMe_2)_2$ (**4d**), as determined by comparison with NMR spectra of an authentic sample.

Reaction of $[(dippe)Rh]_2(\mu\text{-H})_2$ (1) with $Ph_2SiH-HSiPh_2$. To a dark green solution of $[(dippe)Rh]_2(\mu\text{-H})_2$ (**1**; 37 mg, 0.051 mmol) in toluene (5 mL) in a small reactor bomb was added 1,1,2,2-tetraphenyldisilane (prepared from Ph_2SiH_2 using **1** as catalyst; *vide infra*) (19 mg, 0.051 mmol) in toluene (3 mL). Initially there was no color change. The mixture was heated overnight at 70 °C, during which time the solution color changed to red. The toluene was removed under vacuum, and d_6-benzene was added to the residues to make up an NMR sample. The $^{31}P\{^1H\}$ NMR spectrum showed the principal product to be $[(dippe)Rh]_2(\mu\text{-H})(\mu\text{-}\eta^2\text{-H}-SiPh_2)$ (**3a**; 76%). Signals due to small amounts of $[(dippe)Rh]_2(\mu\text{-}SiPh_2)_2$ (**2a**; 13%) and the unknown complex **5** (11%) were also observed. The ^1H NMR spectrum showed the principal silicon-containing product to be 1,1,2,2-tetraphenyldisilane.

Note: Complex **2a**, $[(dippe)Rh]_2(\mu\text{-}SiPh_2)_2$, *does not* react with $Ph_2SiH-HSiPh_2$.

Catalytic Dimerization of Ph_2SiH_2. A typical reaction procedure is as follows: A solution of diphenylsilane (254 mg, 1.38 mmol) in toluene (1.25 mL) was placed in a 50 mL round-bottom flask equipped with a stirbar and condenser. The catalyst (**1**; 0.25 mL of a 0.055 M solution in toluene, 0.014 mmol) was added to the substrate solution by syringe under a strong flow of nitrogen. The solution was degassed by evacuation of the headspace and then heated to 60 °C under nitrogen, open to a bubbler. After 18−24 h the mixture was taken into a glovebox, where the catalyst was removed on a Florisil column. The product mixture was analyzed by ^1H NMR spectroscopy and by GC-MS. ^1H NMR spectra showed the disilane $[Ph_2SiH]_2$ to be the principal product, with yields as high as 78%. Also seen in the spectra were small signals due to unreacted Ph_2SiH_2 and to Ph_3SiH. A small singlet at 4.85 ppm was due to a minor, unidentified product. The GC-MS analysis confirmed the presence of $[Ph_2SiH]_2$, Ph_2SiH_2, Ph_3SiH, and $PhSiH_3$ in these mixtures, but no other peak was observed which might be due to the unidentified product observed in the ^1H NMR spectra. Parent ions (M^+ (*m*/*e*)) observed for these products in the mass spectra are 107 ($PhSiH_3$), 184 (Ph_2SiH_2), 260 (Ph_3SiH), and 366 ($[PhSiH_2]_2$).

Because the solvent (toluene) was removed from the reaction mixture under vacuum, no $PhSiH_3$ (bp 120 °C) was detected in the ^1H NMR spectra. The disilane $[Ph_2SiH]_2$ could be separated from these reaction mixtures by recrystallization from hexanes.

The dimerization reaction does proceed at room temperature, but with lower yields of disilane.

Progress of Reaction Monitored by ^1H NMR. In the glovebox, a solution of diphenylsilane (126 mg, 0.68 mmol) in d_6-benzene (3 mL) was placed in a 250 mL thick-walled reactor bomb, with a small stirbar. The bomb was taken out of the glovebox and attached to a vacuum line. The catalyst solution was also prepared in the glovebox: $[(dippe)Rh]_2(\mu\text{-H})_2$ (**1**; 10 mg, 0.014 mmol) in d_6-benzene (1 mL; a 50:1 substrate-to-catalyst ratio). The dark green catalyst solution was added to the substrate by syringe under a flow of nitrogen. The mixture immediately changed from clear to orange and then within 30 s lightened to yellow. The bomb was left open to the nitrogen manifold and bubbler throughout the experiment. Samples were withdrawn periodically by syringe and analyzed by ^1H NMR spectroscopy, the first being taken 5 min after addition of the catalyst to the substrate and the final being taken 3 h later. The final ^1H NMR spectrum showed a 19% yield of $[Ph_2SiH]_2$.

Calculation of $\Delta G^{\ddagger}$ for the Phosphine and Hydride Exchange in 4d. $\Delta G^{\ddagger}$ was calculated using the value for the rate constant[37] k_C (where $k_C = \pi\Delta\nu_C/(2)^{1/2}$) in the Eyring equation

$$\Delta G^{\ddagger} = -RT_C \ln[(k_C h)/(k_B T_C)]$$

where R = gas constant, T_C = temperature of coalescence, $\Delta\nu_C$ = peak separation at the low-T limit, h = Planck's constant, and k_B = Boltzmann constant. For the phosphorus resonances

(37) Thomas, W. A. *Annu. Rev. NMR Spectrosc.* **1968**, *1*, 43.

in the variable-temperature $^{31}P\{^1H\}$ NMR spectra of **4d**, T_c = 244 K (−29 °C) and $\Delta\nu_c$ = 1590 Hz. For the hydride resonances in the variable-temperature ^1H NMR spectra of **4d**, T_c = 234 K (−39 °C) and $\Delta\nu_c$ = 705 Hz. The coalescence temperatures were estimated visually from the spectra and have an error of approximately ±5 K.

X-ray Crystallographic Analyses of [(dippe)Rh]$_2$(μ-SiRR′)$_2$ (R = R′ = Ph, 2a; R = Ph, R′ = Me, 2b) and [(dippe)Rh(H)]$_2$(μ-η²-H−SiMe$_2$)$_2$ (4d). Crystallographic data appear in Table 1. The final unit-cell parameters were obtained by least squares on the setting angles for 25 reflections with 2θ = 10.9−24.6, 26.5−29.4, and 35.2−40.6°, respectively, for **2a**, *trans*-**2b**, and **4d**. The intensities of 3 standard reflections, measured every 200 reflections throughout the data collection, decayed linearly by 6.4% for **2a** and showed only small random fluctuations for *trans*-**2b** and **4d**. The data were processed[38] and corrected for Lorentz and polarization effects, decay (for **2a**), and absorption (empirical, based on azimuthal scans).

The structure analysis of **2a** was initiated in the centrosymmetric space group $C2/c$ and that of *trans*-**2b** in the centrosymmetric space group $P\bar{1}$ on the basis of the E statistics, these choices being confirmed by subsequent calculations. The structures were all solved by the Patterson method. Molecules of **2a** and *trans*-**2b** have exact (crystallographic) C_2 and C_i symmetry, respectively. The C(6) isopropyl group of **2a** displays high thermal motion and is probably disordered, but no attempts were made to refine a disordered model. Geometrical parameters for this moiety consequently deviate from expected values. One isopropyl carbon atom of **4d** (C(16)) was modeled as (68:32) 2-fold disordered. All non-hydrogen atoms were refined with anisotropic thermal parameters. The metal-bound hydrogen atoms in **4d** were refined with isotropic thermal parameters, and all remaining hydrogen atoms were fixed in calculated positions with C−H = 0.98 Å and $B_H = 1.2B_{\text{bonded atom}}$. Secondary extinction corrections were applied for *trans*-**2b** and **4d** (Zachariasen type, isotropic), the final values of the extinction coefficients being $[9.2(2)] \times 10^{-7}$ and $[4.4(1)] \times 10^{-8}$, respectively. No extinction correction was necessary for **2a**. Neutral atom scattering factors and anomalous dispersion corrections were taken from ref 39. A parallel refinement of the mirror image of **4d** gave substantially higher residuals (R = 0.028 and R_w = 0.030), thus establishing the absolute configuration for the particular crystal used for data collection.

Selected bond lengths and bond angles for **2a**, *trans*-**2b**, and **4d** appear in Tables 2−4, respectively. Tables of final atomic coordinates and equivalent isotropic thermal parameters, anisotropic thermal parameters, bond lengths and angles, torsion angles, intermolecular contacts, and least-squares planes are included as Supporting Information.

Acknowledgment. Financial support for this work was provided by the NSERC (operating grants to M.D.F. and a postgraduate scholarship to L.R.). We thank Johnson-Matthey for a generous loan of $RhCl_3 \cdot 3H_2O$.

Supporting Information Available: Complete tables of non-hydrogen and rhodium hydride parameters, bond lengths and angles, calculated hydrogen atom parameters, anisotropic thermal parameters, torsion angles, and intermolecular contacts and least-squares planes for **2a,b** and **4d**. This material is available free of charge via the Internet at http://pubs.acs.org.

OM980651S

(38) TEXSAN: Structure Analysis Package; Molecular Structure Corp., The Woodlands, TX, 1992.

(39) (a) *International Tables for X-ray Crystallography*; Kynoch Press: Birmingham, U.K. (present distributor Kluwer Academic: Boston, MA), 1974; Vol. IV, pp 99−102. (b) *International Tables for Crystallography*; Kluwer Academic: Boston, MA, 1992; Vol. C, pp 200−206.